Atmos. Chem. Phys. Discuss., 13, 29447–29481, 2013
www.atmos-chem-phys-discuss.net/13/29447/2013/
doi:10.5194/acpd-13-29447-2013

Atmospheric Chemistry and Physics Discussions

Stratospheric ozone depletion from future nitrous oxide increases

W. Wang[1,*], W. Tian[1], S. Dhomse[2], F. Xie[3], and J. Shu[4]

[1]College of Atmospheric Sciences, Lanzhou University, Lanzhou, China
[2]Institute for Climate and Atmospheric Science, School of Earth and Environment, University of Leeds, Leeds, UK
[3]Institute of Atmospheric Physics, Chinese Academy of Sciences, Beijing, China
[4]Institute of Plateau Meteorology, China Meteorological Administration, Chengdu, China
[*]now at: Freie Universität Berlin, Institut für Meteorologie, Berlin, Germany

Received: 8 August 2013 – Accepted: 29 October 2013 – Published: 12 November 2013

Correspondence to: W. Tian (wstian@lzu.edu.cn)

Published by Copernicus Publications on behalf of the European Geosciences Union.

Abstract

We have investigated the impact of assumed nitrous oxide (N_2O) increases on stratospheric chemistry and dynamics by a series of idealized simulations. In a future cooler stratosphere the net yield of NO_y from a changed N_2O is known to decrease, but NO_y can still be significantly increased by the increase of N_2O. Results with a coupled chemistry-climate model (CCM) show that increases in N_2O of 50 %/100 % between 2001 and 2050 result in more ozone destruction, causing a reduction in ozone mixing ratios of maximally 6 %/10 % in the middle stratosphere at around 10 hPa. This enhanced destruction could cause an ozone decline in the second half of this century in the middle stratosphere. However, the total ozone column still shows an increase in future decades, though the increase of 50 %/100 % in N_2O caused a 2 %/6 % decrease in TCO compared with the reference simulation. N_2O increases have significant effects on ozone trends at 20–10 hPa in the tropics and at northern high latitude, but have no significant effect on ozone trends in the Antarctic stratosphere. The ozone depletion potential for N_2O in a future climate depends both on stratospheric temperature changes and tropospheric N_2O changes, which have reversed effects on ozone in the middle and upper stratosphere. A 50 % CO_2 increase in conjunction with a 50 % N_2O increase cause significant ozone depletion in the middle stratosphere and lead to an increase of ozone in the upper stratosphere. Based on the multiple linear regression analysis and a series of sensitivity simulations, we find that the chemical effect of N_2O increases dominates the ozone changes in the stratosphere while the dynamical and radiative effects of N_2O increases are insignificant on average. However, the dynamical effect of N_2O increases may cause large local changes in ozone mixing ratios, particularly, in the Southern Hemisphere lower stratosphere.

1 Introduction

Stratospheric ozone destruction involves complex chemical reactions and a range of chemical species. The catalytic destruction by reactive chlorine and bromine has accounted for a large part of the ozone loss in the stratosphere over the past few decades (WMO, 2007). However, the stratospheric chlorine and bromine loading is now decreasing due to reductions of emissions of anthropogenic chlorofluorocarbons (CFCs) and other halogen-containing chemicals mandated by the Montreal Protocol. Therefore, the effects of other ozone-depleting substances (ODSs) have become a subject of renewed concern in recent years (Wuebbles and Hayhoe, 2002; Chipperfield, 2003; Dentener et al., 2005; Stenke and Grewe, 2005; Ravishankara et al., 2009; Tian et al., 2009). Among these other chemical species, nitrous oxide has been recognized as an important substance affecting stratospheric ozone, and the effect of N_2O on ozone depletion has been discussed in a number of studies (e.g. Crutzen, 1976; Crutzen and Ehhalt, 1977; Kinnison et al., 1988; Randeniya et al., 2002; Chipperfield, 2003). Crutzen and Ehhalt (1977) first pointed out that the increasing use of fixed nitrogen as fertilizer might result in a reduction of the Earth's ozone layer of a few percent at the beginning of the 21st century. Portmann and Solomon (2007) found that increasing N_2O could lead to 2–4 % decline of total column ozone (TCO) by the end of this century under the IPCC A2 scenario. Ravishankara et al. (2009) re-opened the debate on the importance of nitrous oxide for ozone depletion when they argued that N_2O is now the single most important anthropogenic ODSs compared with those regulated by the Montreal Protocol and its amendments.

On the other hand, since the loss of ozone is inversely related to local temperature changes throughout most of the stratosphere, increases in other GHGs such as CO_2 in the future climate also have a large impact on chemical processes in the stratosphere. The effect of N_2O on the ozone layer is not only related to N_2O emission changes but is also modulated by the radiative cooling caused by other GHG emission changes (Rosenfield et al., 2002; Chipperfield, 2009; Wuebbles, 2009; Dameris, 2010). The efficiency of N_2O for global ozone depletion is expected to decrease in the stratosphere due to projected increases in CO_2 (Rosenfield and Douglass, 1998). Some other studies argued that CO_2-induced cooling could cause stratospheric ozone to recover to values greater than 1980 levels during this century (Chipperfield, 2009; Wuebbles, 2009) and lead to a so-called "super recovery". Fleming et al. (2011) further carried out a comprehensive study of long-term stratospheric effects of some source gases including N_2O and CO_2 through series of two-dimensional (2-D) chemistry-climate model simulations. They predicted that in the latter half of the 21st century CO_2, N_2O, and CH_4 loading will all have significant impacts on global total ozone while the effect of CO_2 loading on global total ozone has twice the magnitude of the effect of N_2O.

Although previous studies have investigated the impact of N_2O on ozone depletion, the relative importance of the radiative and chemical effect of N_2O remains unclear and the net effect of increased N_2O on the ozone layer in the changing climate is still under debate. Previous studies have mostly been based on mechanistic analysis, with the main focus being the chemical effect of N_2O (Ravishankara et al., 2009), or have used relatively simple two-dimensional chemical-dynamical models (e.g. Portmann and Solomon, 2007; Chipperfield, 2009; Fleming et al., 2011) to diagnose the effect of N_2O changes on the ozone layer. In this study, we re-examine the effect of N_2O increases on ozone using a fully coupled 3-D chemistry-climate model (CCM). We attempt to clarify quantitatively the radiative and chemical effects of N_2O increases on the ozone layer and to diagnose the ozone changes in a changing climate when CO_2 and N_2O are both increasing. The details of the model and numerical experiments are given in Sect. 2. The effect of N_2O increases on ozone depletion under different scenarios is addressed in Sect. 3. In Sect. 4, we analyze contributions of various factors associated with N_2O increases in modulating ozone depletion. Conclusions and a discussion are presented in Sect. 5.

2 Models and numerical experiments

We have used a fully coupled chemistry-climate model, the Whole Atmosphere Community Climate Model 3 (WACCM3) to investigate the chemical and thermal-dynamical responses to a linear future increase in N_2O. WACCM3 has 66 vertical levels from the ground to 4.5×10^{-6} hPa (approximately 145 km geometric altitude) with detailed interactive chemistry (Garcia et al., 2007) and a finite volume dynamical core (Lin, 2004). For this study simulations were carried out at $4^\circ \times 5^\circ$ horizontal resolution. The WACCM3 chemistry module is derived from the three-dimensional (3-D) chemical transport Model for Ozone and Related chemical Tracers (MOZART) (Brasseur and Hitchman, 1988; Hauglustaine et al., 1998; Horowitz et al., 2003). More details of WACCM3 model can be found in Garcia et al. (2007).

Four long-term WACCM simulations were performed in this study and detailed configurations of those simulations are listed in Table 1. The surface volume mixing ratios (vmrs) of GHGs in the control run (E0) are taken from IPCC A1b scenario. In runs E1 and E2, the surface vmrs of N_2O were increased linearly with time from 2001 to 2050 at a rate of 1 % yr^{-1} in run E1 and 2 % yr^{-1} in run E2. More specifically, N_2O values in E1 are increased by 1 % in 2001, 2 % in 2002, and 50 % in 2050. It should be pointed out that the percentage increases of N_2O in each year are based on N_2O values of A1B scenario. For instance, in year 2050, N_2O value of A1B scenario is 344 ppbv in run E0, therefore, it is 517 ppbv in run E1 and 688 ppbv in run E2. This increasing approach makes the N_2O variation in our simulations close to A1B scenario during the first half of the simulations with small additional increases in each year compared to A1B scenario, but far off A1B scenario with much larger N_2O increases during the later half of the simulations for the purpose of amplifying response signals of the atmosphere. In run E3, both N_2O and CO_2 are increased linearly with time from 2001 and increased by 50 % in 2050 with an increasing rate of 1 % yr^{-1}. The sea surface temperature (SST) and sea ice fields used in four runs are the same (HadGEM1) and derived from the SST and sea ice fields prepared for the Chemistry-Climate Model Validation activity 2

(CCMVal-2) REF2 simulations (Eyring et al., 2008; Morgenstern et al., 2010) for the period 2001 to 2050.

To separate the radiative and chemical effects of increasing N_2O on stratospheric ozone, 4 extra WACCM time-slice simulations were performed. In the first simulation (S0), GHG loadings were based on the IPCC A1b scenario and fixed at the year 2050 in both the chemistry and radiation scheme. In simulations S1 and S2, N_2O mixing ratios were increased by 50 % relative to that in simulation S0 in the model's chemistry and radiation schemes, respectively. In the last simulation S3, N_2O was increased by 50 % relative to that in simulation S0 in both the chemistry and radiation schemes. All of these sensitivity simulations used 12 month SST and sea ice climatology derived from observed monthly mean values for the time period from 1996 to 2000 (Rayner et al., 2003).

3 Results

3.1 Ozone responses to N_2O changes in a CCM

Figure 1 shows percentage changes of ozone mixing ratio and total column ozone (TCO) caused by N_2O increases. These ozone changes are calculated from the climatology of the final 10 yr (2041–2050) of the four WACCM runs listed in Table 1. It is apparent from Fig. 1 that the ozone changes have large spatial and temporal variations. In the middle and upper stratosphere, a decrease of 6–10 % ozone occurs when N_2O increases by 50 %/100 % (Fig. 1a and b).

In the middle and upper stratosphere, N_2O decomposes by photolysis or by reactions with $O(^1D)$:

$$N_2O + h\upsilon \rightarrow N_2 + O \quad \text{(R1)}$$

$$N_2O + O(^1D) \rightarrow N_2 + O_2 \quad \text{(R2)}$$

$$N_2O + O(^1D) \rightarrow 2NO \quad \text{(R3)}$$

Only the minor channel of Reaction (R3) leads to NO_y (= NO_x + NO_3 + HNO_3 + HO_2NO_2 + $ClONO_2$ + $2N_2O_5$ + $BrONO_2$ +...) production. NO_y is removed from the stratosphere by transport to the troposphere and washout or by local photochemical loss at high altitudes via:

$$N + NO \rightarrow N_2 + O \quad k_4 = 2.1 \times 10^{-11} \exp(+100/T) \tag{R4}$$

The abundance of N is determined by photolysis of NO and by the reaction:

$$N + O_2 \rightarrow NO + O_2 \quad k_5 = 1.5 \times 10^{-11} \exp(-3600/T) \tag{R5}$$

Because of the temperature dependence of the reactions controlling the chemical loss of NO_y, NO_y tends to decrease in a future cooler stratosphere as Reaction (R4) speeds up while Reaction (R5) slows down (Rosenfield and Douglass, 1998). Without significant stratospheric cooling, N_2O increases in the atmosphere will cause NO_y and NO_x increases in the stratosphere. Figure 2 shows the time series of global mean NO_x and NO_y fields from the four experiments and corresponding changes in global mean column NO_x and NO_y in runs E1, E2 and E3 relative to that in control run E0. Note that a 100 % increase in N_2O by the end of 2050 causes an increase in the global mean column NO_y and NO_x by 12×10^{15} molecules cm^{-2} and 4×10^{15} molecules cm^{-2} , respectively. However, when CO_2 is also increased by 50 % in conjunction with a 50 % N_2O increase at the end of 2050 in run E3, which implies a cooler stratosphere than that in run E1 in which only N_2O is increased by 50 % at the end of 2050, the NO_y and NO_x increases are smaller than those in run E1 (Fig. 1a and c). Even though the yield of NO_x from N_2O decreases in a cooler stratosphere, the efficiency of ozone loss due to NO_y increases so that N_2O increases in run E3 still causes an increase in ozone loss due to the increasing NO_y in an atmosphere with decreasing halogens. These results imply that the ozone depletion potential for N_2O in a future climate will actually depend both on stratospheric temperature changes and tropospheric N_2O changes, which have reversed effects on ozone in the middle and upper stratosphere. Figure 1 clearly indicates that the destruction of ozone associated with N_2O increases in run E3

is reduced relative to that in runs E1, particularly in the middle and upper stratosphere, consistent with previous findings that CO_2-induced cooling tends to increase ozone in the future (e.g. Haigh and Pyle, 1982; Shepherd, 2008; Chipperfield, 2009; Wuebbles, 2009; Oman et al., 2010a) by slowing down the gas-phase chemical reactions associated with ozone.

In the lower stratosphere, increased N_2O could reduce the efficiency of Cl_y and Br_y for ozone destruction by tying up more of these halogens in the $ClONO_2$ and $BrONO_2$ reservoir species, consequently, N_2O increases lead to more ozone. Meanwhile, projected decreases in Cl_y and Br_y tend to tie up less NO_y in $ClONO_2$ and $BrONO_2$, and increase the efficiency of N_2O in ozone destruction processes (e.g. Ravishankara et al., 2009; Daniel et al., 2010), but Fig. 1 suggests that this effect is outweighed by the effect of N_2O increases. On the other hand, in the lower stratosphere/upper troposphere UV radiation is enhanced due to the ozone decreases in the middle and upper stratosphere, resulting in more ozone production through the so-called "self-healing" effect. A notable feature in Fig. 1 is that this ozone increase in the lower stratosphere/upper troposphere can be seen mostly at Southern Hemisphere mid-latitudes. Ravishankara et al. (2009) pointed out that the "self-healing" effect is most significant at tropical latitudes. As will be discussed later, this significant ozone increase in the Southern Hemisphere is partly caused by the enhanced vertical transport of ozone from the upper atmosphere to the lower stratosphere/upper troposphere, which may not be well simulated in 2-D models. Below 100 hPa in the troposphere, N_2O increases result in more ozone with a maximum 10 % increase at southern high latitudes when N_2O is increased by 100 % from 2001 to 2050 (Fig. 1b).

Due to significant ozone decreases in the middle and upper stratosphere caused by increased N_2O, the TCO in the two WACCM simulations (E1 and E2) decreases compared with control run E0 (Fig. 1d and e), particularly at high latitudes. A 50 % increase in N_2O causes a maximum 6 % decrease in TCO (Fig. 1d). When N_2O is increased by 100 % in run E2, TCO changes become larger with a maximum decrease of 10 % at high latitudes. The combined effect of N_2O and CO_2 increases results in

a slight TCO decrease (1–2 %) in the Northern Hemisphere but an increase (2–6 %) in the Southern Hemisphere (Fig. 1f), due to the offsetting impact of CO_2-induced cooling.

Figure 3a–c shows modeled ozone trends as a function of latitude and pressure from 2000 to 2050 under different assumed N_2O changes. Also shown are the time series of TCO averaged over different latitude bands, i.e., 90° N–70° N, 22° S–22° N, and 70° S–90° S. Consistent with results in previous studies (e.g. Tian and Chipperfield, 2005; Austin and Wilson, 2006; Newman et al., 2006; Eyring et al., 2007; WMO, 2007), the global ozone will generally recover in the next half century under the IPCC A1b GHGs scenario with a maximum increasing trend of 0.3 ppmv/10 yr at 10–1 hPa (Fig. 3a). However, if N_2O is further increased by 50 % relative to the IPCC A1b projection, the ozone in the middle stratosphere at around 20 hPa decreases with a maximum trend of −0.2 ppmv/10 yr, although the ozone in the upper stratosphere still increases (Fig. 3b). Note that a steadily declining trend in ozone in the tropical lower stratosphere was also simulated in previous simulations (Oman et al., 2010a; SPARC-CCMVal, 2010; Eyring et al., 2010a), but there is no significant ozone trend in the tropical lower stratosphere in our simulations through 2050. A possible reason is that the upwelling in our 50 yr simulations has not significantly increased in the lower stratosphere/upper troposphere (Table 3) though we used an increased GHG scenario and time varying SSTs. As in Fig. 1, CO_2 increases tend to offset the effect of N_2O on ozone trends in the middle stratosphere (Fig. 3c). When N_2O and CO_2 are both increased by 50 %, the declining trend of ozone in the middle stratosphere becomes less significant. It is worth noting that the effect of increased N_2O on long-term trends of ozone mixing ratios at about 20–10 hPa have evident spatial variations. Ozone mixing ratios decrease most significantly in the tropics with a trend up to −0.1 ppmv/10 yr when N_2O is increased by 50 %. N_2O increases have no significant effect on ozone trends in the Antarctic stratosphere but tend to slow down the ozone recovery in the Arctic stratosphere. Previous studies also found that ozone evolution over Antarctic shows small sensitivity to changes in GHGs (Eyring et al., 2010a). Similar features can be noted in the TCO time series shown in Fig. 3d–f. Figure 3 also indicates that the higher N_2O corresponds to a less

significant increasing trend of ozone, implying that increased N_2O overall tends to delay the recovery of ozone.

To understand the hemispheric asymmetry of ozone trends in the middle stratosphere exhibited in Fig. 3, Fig. 4 shows the time series of ozone mixing ratios averaged over different latitude bands between 20–10 hPa. Also shown are the corresponding time series of the reactive chlorine (ClO_x, ClO_x = Cl + ClO + $2Cl_2O_2$). Generally, in all simulations ClO_x tends to decrease in response to the decreasing chlorine loading due to the Montreal Protocol and its amendments, which is imposed in the model through specified surface halocarbon mixing ratios. However, the relative rates of ClO_x decline between experiments are different. In the Arctic stratosphere ClO_x tends to increase with increased N_2O in the first half of the simulations and then reverses in the second half. In the Antarctic middle stratosphere, N_2O increases have no significant effect on ClO_x, which shows an evident decreasing trend with marginal differences between the four experiments. Accordingly, the ozone time series in the Antarctic middle stratosphere show persistent increasing trends in all four experiments.

A further examination of the model chemical fields reveals that NO_x concentrations in the Antarctic stratosphere are lower than those in the Arctic stratosphere (not shown), and the differences become larger when the additional N_2O increases from 50 % to 100 %. As discussed below (see Fig. 6), in the Arctic higher odd nitrogen values from increased N_2O lead to more PSC occurrence which results in more ozone loss. Meanwhile in the Antarctic PSC occurrence does not change from our model simulations. Those effects of N_2O increases on ozone between 20–10 hPa are evident in Fig. 1a, c which show that ozone concentrations in the Arctic stratosphere tend to decrease when N_2O is increased, but in the Antarctic stratosphere, ozone still exhibits an increasing trend.

3.2 Thermal-dynamical feedbacks associated with N_2O increases

The effect of N_2O increases on ozone in the tropical stratosphere is not only related to chemical processes. Austin et al. (2010a) pointed out that the strengthened Brewer–

Dobson (BD) circulation in the future climate could lead to ozone decreases in the tropical lower stratosphere as a result of intensified upward transport of ozone-poor air from below. Table 3 lists the tropical (25° N–25° S) upwelling (w^*) at 70–20 hPa averaged over the last 10 yr of the 4 WACCM experiments, and its change (δw^*) relative to the first 10 yr of simulations. It is apparent that the tropical upwelling increases with increased GHGs. However, one can see that relative changes of w^* between the first and last decade of the simulations do not vary simply with GHG loading. In the experiment with both N_2O and CO_2 increases (run E3), δw^* is not even the largest. This is consistent with the result in Xie et al. (2008) who showed that without SST increases associated with GHGs increases, the change in the tropical upwelling is not significant. Note that there is only very small value for δw^* in our reference run (E0), which is a possible reason for the small ozone declining trend in the tropical lower stratosphere. It is known that the tropical upwelling is increasing in a warming climate. It is interesting that the trend in the tropical upwelling in our reference run is insignificant. A careful examination of the trends of the SSTs used in our simulation reveals that the SST trends are relatively weak compared with those of CCSM3 SST data which are widely used in CCM simulations in previous studies (SPARC-CCMVal, 2010). This may be the possible reason for the short of significant increases in the tropical upwelling in our reference run (E0).

As a greenhouse gas, N_2O increases can directly warm the troposphere and can also influence stratospheric temperature, by the direct radiative effect and by the indirect radiative effect associated with ozone feedbacks. Figure 5 shows the modeled temperature changes caused by different N_2O increases. A 50 % increase of N_2O causes a 1 K cooling in the northern middle stratosphere and a 2 K cooling above 1 hPa at southern high latitudes (Fig. 5a). A 100 % increase in N_2O causes a cooling in most regions of the stratosphere, with a maximum 3 K cooling in the tropical middle stratosphere (Fig. 5b). By comparing Figs. 3 and 5, we can see that the impact of N_2O on stratospheric temperatures is mainly caused by N_2O-induced ozone changes, rather than the direct radiative effect of N_2O. As expected, the cooling of the stratosphere

becomes much larger when CO_2 is also increased by 50 % together with a 50 % N_2O increase (Fig. 5c). Also shown in Fig. 5 are the water vapor changes between the WACCM runs. Stratospheric water vapor depends on tropopause temperatures and production from CH_4 oxidation. As temperature changes in the upper troposphere and lower stratosphere (UTLS) region (Fig. 5a–c), a general decrease of water vapor on the order of 0.05 ppmv is simulated in the upper stratosphere and a significant increase of 0.15 ppmv can be noted in the mid-latitude lower stratosphere in the SH if N_2O is increased by 50 %. When N_2O is increased by 100 %, water vapor increases in the atmosphere due to warming of the tropopause, as is evident in Fig. 5b. Due to the significant cooling of the stratosphere caused by CO_2 and N_2O increases, the stratospheric water vapor decreases in run E3 (Fig. 5f).

Stratospheric methane and water vapor are closely related through chemical oxidation and dynamical transport processes. Figure 5g, h, j show the CH_4 changes caused by N_2O and CO_2 increases. Throughout the stratosphere, water vapor changes are anti-correlated with methane changes. More CH_4, which is shown as a round 0.05–0.07 ppmv in the middle to upper stratosphere (10 hPa to 1 hPa) and maximises in the tropics, is transported to the middle and upper stratosphere as a result of an enhanced BD circulation in response to N_2O and CO_2 increases. Compared with CH_4 increases in E1, in which N_2O is increased by 50 % (Fig. 5g), the CH_4 increases seem to be smaller in magnitude when N_2O increased by 100 % in run E2 (Fig. 5h). This is partly caused by transport differences in the tropical lower stratosphere between runs E1 and E2, since the BD circulation in E2 is stronger than that in E1. Also, a more significant decrease of CH_4 can be found in E2 in the lower stratosphere compared with in E1. CH_4 is oxidized by reactions involving OH, $O(^1D)$ and Cl radicals (e.g. Röckmann et al., 2004), which are perturbed by the GHG increases. The non-linear responses of CH_4 to N_2O increases indicate that the changes in CH_4 are due to the competing effects of transport and chemistry.

As polar stratospheric clouds (PSCs) are closely related to ozone loss in the polar stratosphere (e.g. Rex et al., 2004; Chipperfield et al., 2005; Austin et al., 2010b), it

is useful to examine the effect of N_2O increases on the occurrence of PSCs. Figure 6 shows the vertical distribution of the modeled change in the PSC surface area in the Antarctic and Arctic. The modeled PSC area is enlarged by 1–2 × 10^6 km^2 in the Arctic between 200 and 20 hPa, when N_2O is increased by 50–100 %. In the Antarctic lower stratosphere, however, N_2O increases cause no significant changes in the moddled PSC area. An exception occurs in the Antarctic mid-stratosphere at about 10 hPa, at the upper limit of PSC occurrence, where additional cooling can cause more PSCs. Figure 6 suggests that the N_2O increases have a different impact on the modeled PSC area in the Arctic and Antarctic stratosphere. In the Arctic stratosphere, temperatures are close to the threshold for widespread PSC formation and the cooling caused by N_2O increases can result in more PSCs. In the Antarctic lower stratosphere, temperatures in winter and spring are essentially always low enough for PSC formation, therefore, a small cooling caused by N_2O increases has no significant impact on PSC formation. This difference in the change in modeled PSC area between the Arctic and Antarctic makes a significant contribution to the hemispheric asymmetry of ozone destruction discussed in Fig. 3. However, previous studies (SPARC-CCMVal, 2010) showed that the potential for chlorine activation (PACl) in the Arctic simulated by WACCM is overall larger than expected, though it performs well for polar ozone depletion processes. This may lead to an overestimate for the ozone depleting effects of N_2O increases in the Arctic. Also noticeable is that compared to run E1, the impact of an additional 50 % N_2O increase (run E2) causes a larger increase in PSC area in the Arctic than an additional 50 % CO_2 increase. Here the increased NO_y from N_2O promotes the formation of nitric acid trihydrate.

4 Contributions to ozone depletion from different factors due to N_2O changes

The attribution of ozone variations to dynamical, radiative, and chemical effects resulting from changes in GHGs and ODSs is an important problem in stratospheric climate. Multiple linear regression (MLR) is typically used to estimate statistical model parameters (e.g. WMO, 2007; Shepherd, 2008; Stolarski et al., 2010; Oman et al., 2010b). For a given location and time, an ozone change (ΔO_3) can be expressed as follows:

$$\Delta O_3(t) = \sum_j c_j \Delta X_j(t) + \varepsilon(t) \quad (1)$$

where the variables X_j are the factors that can affect ozone, the coefficients c_j are the sensitivity of ozone to the factor X_j, and ε is the error in the fit. Here, ΔO_3 and ΔX_j are the changes in ozone and other quantities between different model experiments with respect to the control experiment (E0) (i.e., $\Delta O_3 = O_{3,E1} - O_{3,E0}$, where $O_{3,E1}$ and $O_{3,E0}$ represent modeled ozone data from runs E0 and E1, respectively).

We select NO_x, ClO_x, as well as temperature (T) as proxies to represent the direct chemical effect, indirect chemical effect and radiative effect result from N_2O increases, respectively. Reactive hydrogen (HO_x) and transport parameters are not included, since their effects are relatively small (not shown). The MLR analysis described above is performed on the modeled data from the control run E0 and run E1, in which N_2O is increased by 50 % by 2050. Ozone changes (ΔO_3) caused by the selected regression factors are examined over different latitude bands (i.e., 90° N–70° N, 22° N–22° S, and 70° S–90° S) on all the model levels from surface to 1 hPa, and the results are shown in Fig. 7.

The contributions of different factors to ozone changes are strongly latitude and altitude dependent. In the Arctic, NO_x and temperature changes cause ozone decreases in the lower and middle stratosphere. NO_x changes, which represent the direct chemical effect of N_2O increases, contribute over 80 % or even higher to the 0.5 ppmv ozone decrease from 70 to 10 hPa (Fig. 7a). Figure 7a also shows that in the upper stratosphere, ClO_x changes result in more ozone. In the tropics (Fig. 7b) both temperature and ClO_x changes tend to result in more ozone in the mid-upper stratosphere. NO_x changes lead to large ozone depletion (about 150 % of total ozone changes) which are partly offset (about 50 %) by the T and ClO_x contributions. NO_x changes in the lower stratosphere cause more ozone on the order of 0.2 ppmv, while ClO_x and T have no

significant effects on ozone there. The contribution of NO_x to ozone changes, which peaks at 10–3 hPa, is consistent with earlier studies (Oman et al., 2010b; Eyring et al., 2010b). In the Antarctic (Fig. 7c) the ozone changes caused by NO_x changes are still negative but relatively small compared to those in the tropical and Arctic stratosphere. In contrast to those in the Arctic stratosphere, ozone changes associated with ClO_x are negative in the Antarctic stratosphere. Note also that temperature has a more significant contribution on ozone changes than NO_x in the Antarctic stratosphere. Similar features can be obtained when MLR analysis is performed on the modeled data from control run E0 and run E2 in which N_2O is increased by 100 % by 2050 (not shown).

This multiple regression analysis suggests that the direct chemical effect (indicated by NO_x) of N_2O on ozone changes contributes to the largest part of ozone changes in the lower stratosphere, while the indirect chemical effect (indicated by ClO_x) of N_2O, which is associated with enhanced chlorine-catalyzed ozone destruction, is more important in the upper stratosphere. The effect of temperature changes (indicated as T) is more pronounced in the tropical upper stratosphere but relatively less significant in the polar stratosphere. It should be pointed out that some non-linear or interdependent effects of N_2O increase on ozone, such as ozone depletion associated with PSCs, may not be well separated by the MLR analysis. Nevertheless, it provides us with some useful information on the contributions of different processes associated with N_2O increases to ozone changes.

We now discuss the results of the WACCM sensitivity runs which applied N_2O increases separately to the model's radiation and chemistry schemes. The changes in ozone and temperature caused by chemical and radiative effects of N_2O increases are shown in Fig. 8. Ozone decreases up to 10 % (1 ppmv) (Fig. 8a) when the 50 % N_2O increase is applied to the chemistry routine, while the same increase of N_2O in the radiation scheme causes no more than 1 % (0.1 ppmv) ozone decrease (Fig. 8b). When N_2O is increased in both the chemistry and radiation schemes, the ozone changes show no significant differences from those caused by the chemical effect of a 50 % N_2O alone (not shown). It is clear that the chemical effect contributes most to the ozone changes

caused by N_2O increase, which is consistent with the MLR analysis. The ozone depletion causes significant subsequent stratospheric cooling, with a maximum of −1.7 K in the middle stratosphere (around 10 hPa) in the tropics (Fig. 8c). The direct radiative effect of N_2O is much smaller (below 1 K) than the indirect radiative effects (Fig. 8c and d) without a clear pattern in the spatial distribution.

Another factor which should also be considered is the dynamical effect of increasing N_2O. As shown in Table 3, the increase in N_2O is likely to strengthen the BD circulation. Meanwhile, this strengthened circulation influences the distribution and also contributes to the variability of O_3. Figure 9 shows the vertical ozone flux in the reference experiment E0 (Fig. 9a) as well as the corresponding changes in E1 relative to that in control run E0 (Fig. 9b). For a given grid cell $A[\mathrm{lat}_i, \mathrm{lev}_k]$ located at the latitude of lat_i and the pressure levels of lev_k, the vertical ozone flux is defined as the incoming ozone at the lower level lev_{k-1} ($O_3[\mathrm{lat}_i, \mathrm{lev}_{k-1}] \times w^*[\mathrm{lat}_i, \mathrm{lev}_{k-1}]$) minus the ozone coming out at higher level $level_{k+1}$($O_3[\mathrm{lat}_i, \mathrm{lev}_{k+1}] \times w^*[\mathrm{lat}_i, \mathrm{lev}_{k+1}]$). Consistent with the overall picture of the BD circulation, the ozone in the tropical lower stratosphere is transported to the upper stratosphere and ozone in the mid-latitude upper stratosphere is transported downward to the lower stratosphere (Fig. 9a). It is evident from Fig. 9b that the strengthened BD circulation caused by the increased N_2O leads to a net decrease of ozone in the tropical lower stratosphere and a net ozone increase at around 100 hPa at southern mid-to-high latitudes. The large ozone increases around 100 hPa at southern mid-latitudes exhibited in Fig. 1a–c may be mainly caused by this transport effect. The MLR analysis with w^* as an additional regression factor suggests that the dynamic effect of a N_2O increase on ozone changes is much less significant than its chemical and radiative effects in most of the areas (not shown). The result here implies that the dynamical effect of increasing N_2O on ozone is small on average, but may have a significant contribution to local ozone changes in the mid-latitude stratosphere.

5 Discussion and conclusions

The distribution of ozone changes resulting from N_2O increases in a 3-D CCM shown as function of latitude and altitude and the chemical mechanism was discussed by examining various chemical species related to ozone destruction. Subsequent climate changes induced by these N_2O increases, such as changes in stratospheric temperatures and water vapor, BD circulation and area of PSCs, were also examined, helping us to understand the N_2O and ozone interactions with climate changes. A series of sensitivity simulations and MLR were performed to detect the dominant factors controlling the ozone changes caused by N_2O increases.

The CCM results suggest that N_2O increases by 50 %/100 % between 2001 and 2050 result in more ozone destruction, reducing in ozone mixing ratios of maximally 6 %/10 % in the middle stratosphere at around 10 hPa. However, the total ozone column still shows an increase in future decades. The increase of N_2O also results in significant temperature and H_2O changes, which are seen in a slight cooling in the stratosphere and an evident increase of stratospheric H_2O. In a future cooler stratosphere the net yield of NO_y is known to decrease, and our simulations indicate that the ozone-depleting impact of N_2O becomes smaller due to the cooling and fewer halogens in the stratosphere. The ozone depletion potential for N_2O in a future climate depends on whether the stratospheric cooling effect is larger than the effect of tropospheric N_2O changes. The increase of N_2O has only a small influence on chemical processes associated with Antarctic ozone destruction. However, increased emissions of N_2O are likely to delay recovery of the ozone in the Arctic stratosphere.

The depletion of ozone caused by nitrous oxide involves complex dynamical, chemical and radiative processes. The analyses based on a series of sensitivity simulations and MLR suggests that N_2O increases cause ozone changes mainly through chemical processes. The direct chemical effect of N_2O increases (via NO_x chemistry) contributes the majority of ozone changes in the lower and middle stratosphere, while the indirect chemical effect of N_2O increases (via halogen chemistry) is simulated as the dominant

factor in ozone depletion in the upper stratosphere. The direct radiative effect of N_2O increases on ozone is very small, but the indirect radiative effect associated with ozone changes is evident and coupled with chemical and dynamical processes. The dynamical effect of increasing N_2O is also small on average, but can cause large local ozone changes in the mid-latitude stratosphere. The ozone depleting effect of N_2O increases can be significantly reduced in the middle stratosphere when CO_2 is also increased, implying that the depletion of ozone caused by N_2O increases depends strongly on stratospheric temperature changes.

Acknowledgements. This work was supported by the National Science Foundation of China (41175042, 41225018) and National Basic Research Program of China (2010CB428604). We also thank the Fundamental Research Funds for the Central Universities of China and the computing resources from Supercomputing Center of Cold and Arid Region Environment and Engineering Research Institute of Chinese Academy of Sciences. We thank John Austin for advice on WACCM experiments, Martyn Chipperfield from the University of Leeds for comments on the manuscript, Lisa Neef from GEOMAR for grammar checking and Shaojie Ma and Guohui Zhao for help in data processing.

References

Austin, J. and Wilson, R. J.: Ensemble simulations of the decline and recovery of stratospheric ozone, J. Geophys. Res., 111, D16314, doi:10.1029/2005JD006907, 2006. 29455

Austin, J., Scinocca, J., Plummer, D., Oman, L., Waugh, D., Akiyoshi, H., Bekki, S., Braesicke, P., Butchart, N., Chipperfield, M., Cugnet, D., Dameris, M., Dhomse, S., Eyring, V., Frith, S., Garcia, R. R., Garny, H., Gettelman, A., Hardiman, S. C., Kinnison, D., Lamarque, J. F., Mancini, E., Marchand, M., Michou, M., Morgenstern, O., Nakamura, T., Pawson, S., Pitari, G., Pyle, J., Rozanov, E., Shepherd, T. G., Shibata, K., Teyssèdre, H., Wilson, R. J., and Yamashita, Y.: Decline and recovery of total column ozone using a multimodel time series analysis, J. Geophys. Res., 115, D00M10, doi:10.1029/2010JD013857, 2010a. 29456

Austin, J., Struthers, H., Scinocca, J., Plummer, D. A., Akiyoshi, H., Baumgaertner, A. J. G., Bekki, S., Bodeker, G. E., Braesicke, P., Brühl, C., Butchart, N., Chipperfield, M. P.,

Cugnet, D., Dameris, M., Dhomse, S., Frith, S., Garny, H., Gettelman, A., Hardiman, S. C., Jöckel, P., Kinnison, D., Kubin, A., Lamarque, J. F., Langematz, U., Mancini, E., Marchand, M., Michou, M., Morgenstern, O., Nakamura, T., Nielsen, J. E., Pitari, G., Pyle, J., Rozanov, E., Shepherd, T. G., Shibata, K., Smale, D., Teyssèdre, H., and Yamashita, Y.: Chemistry-climate model simulations of spring Antarctic ozone, J. Geophys. Res., 115, D00M11, doi:10.1029/2009JD013577, 2010b. 29458

Brasseur, G. and Hitchman, M. H.: Stratospheric response to trace gas perturbations: changes in ozone and temperature distributions, Science, 240, 634–637, doi:10.1126/science.240.4852.634, 1988. 29451

Chipperfield, M.: Atmospheric science: nitrous oxide delays ozone recovery, Nat. Geosci., 2, 742–743, doi:10.1038/ngeo678, 2009. 29449, 29450, 29454

Chipperfield, M., Feng, W., and Rex, M.: Arctic ozone loss and climate sensitivity: updated three-dimensional model study, Geophys. Res. Lett., 32, L11813, doi:10.1029/2005GL022674, 2005. 29458

Chipperfield, M. P.: Comment on: "Stratospheric Ozone Depletion at northern mid-latitudes in the 21st century: the importance of future concentrations of greenhouse gases nitrous oxide and methane", Geophys. Res. Lett., 30, 1389, doi:10.1029/2002GL016353, 2003. 29449

Crutzen, P. J.: Upper limits on atmospheric ozone reductions following increased application of fixed nitrogen to the soil, Geophys. Res. Lett., 3, 169–172, doi:10.1029/GL003i003p00169, 1976. 29449

Crutzen, P. J. and Ehhalt, D. H.: Effects of nitrogen fertilizers and combustion on the stratospheric ozone layer, Ambio, 6, 112–117, 1977. 29449

Dameris, M.: Depletion of the ozone layer in the 21st century., Angew. Chem. Int. Edit., 49, 489–491, doi:10.1002/anie.200906334, 2010. 29449

Daniel, J. S., Fleming, E. L., Portmann, R. W., Velders, G. J. M., Jackman, C. H., and Ravishankara, A. R.: Options to accelerate ozone recovery: ozone and climate benefits, Atmos. Chem. Phys., 10, 7697–7707, doi:10.5194/acp-10-7697-2010, 2010. 29454

Dentener, F., Stevenson, D., Cofala, J., Mechler, R., Amann, M., Bergamaschi, P., Raes, F., and Derwent, R.: The impact of air pollutant and methane emission controls on tropospheric ozone and radiative forcing: CTM calculations for the period 1990-2030, Atmos. Chem. Phys., 5, 1731–1755, doi:10.5194/acp-5-1731-2005, 2005. 29449

Eyring, V., Waugh, D., Bodeker, G., Cordero, E., Akiyoshi, H., Austin, J., Beagley, S., Boville, B., Braesicke, P., Brühl, C., C., Butchart, N., Chipperfield, M. P., Dameris, M., Deckert, R.,

Deushi, M., Frith, S. M., Garcia, R. R., Gettelman, A., Giorgetta, M. A., Kinnison, D. E., Mancini, E., Manzini, E., Marsh, D. R., Matthes, S., Nagashima, T., Newman, P. A., Nielsen, J. E., Pawson, S., Pitari, G., Plummer, D. A., Rozanov, E., Schraner, M., Scinocca, J. F., Semeniuk, K., Shepherd, T. G., Shibata, K., Steil, B., Stolarski, R. S., Tian,W., and Yoshiki, M: Multimodel projections of stratospheric ozone in the 21st century, J. Geophys. Res., 112, D16303, doi:10.1029/2006JD008332, 2007. 29455

Eyring, V., Chipperfield, M., Giorgetta, M., Kinnison, D. E., Manzini, E., Matthes, K., Newman, P., Pawson, S., Shepherd, T., andWaugh, D.: Overview of the new CCMVal reference and sensitivity simulations in support of upcoming ozone and climate assessments and planned SPARC CCMVal, SPARC Newsletter, 30, 20–26, 2008. 29452

Eyring, V., Cionni, I., Bodeker, G. E., Charlton-Perez, A. J., Kinnison, D. E., Scinocca, J. F., Waugh, D. W., Akiyoshi, H., Bekki, S., Chipperfield, M. P., Dameris, M., Dhomse, S., Frith, S. M., Garny, H., Gettelman, A., Kubin, A., Langematz, U., Mancini, E., Marchand, M., Nakamura, T., Oman, L. D., Pawson, S., Pitari, G., Plummer, D. A., Rozanov, E., Shepherd, T. G., Shibata, K., Tian, W., Braesicke, P., Hardiman, S. C., Lamarque, J. F., Morgenstern, O., Pyle, J. A., Smale, D., and Yamashita, Y.: Multi-model assessment of stratospheric ozone return dates and ozone recovery in CCMVal-2 models, Atmos. Chem. Phys., 10, 9451–9472, doi:10.5194/acp-10-9451-2010, 2010a. 29455

Eyring, V., Cionni, I., Lamarque, J. F., Akiyoshi, H., Bodeker, G. E., Charlton-Perez, A. J., Frith, S. M., Gettelman, A., Kinnison, D. E., Nakamura, T., Oman, L. D., Pawson, S., and Yamashita, Y.: Sensitivity of 21st century stratospheric ozone to greenhouse gas scenarios, Geophys. Res. Lett., 37, L16807, doi:10.1029/2010GL044443, 2010b. 29461

Fleming, E. L., Jackman, C. H., Stolarski, R. S., and Douglass, A. R.: A model study of the impact of source gas changes on the stratosphere for 1850–2100, Atmos. Chem. Phys., 11, 8515–8541, doi:10.5194/acp-11-8515-2011, 2011. 29450

Garcia, R. R., Marsh, D. R., Kinnison, D. E., Boville, B. A., and Sassi, F.: Simulation of secular trends in the middle atmosphere, 1950–2003, J. Geophys. Res., 112, D09301, doi:10.1029/2006JD007485, 2007. 29451

Haigh, J. and Pyle, J.: Ozone perturbation experiments in a two-dimensional circulation model, Q. J. Roy. Meteor. Soc., 108, 551–574, doi:10.1002/qj.49710845705, 1982. 29454

Hauglustaine, D., Brasseur, G., Walters, S., Rasch, P., Müller, J.-F., Emmons, L., and Carroll, M.: MOZART, a global chemical transport model for ozone and related chemical tracers: 2. Model

results and evaluation, J. Geophys. Res., 103, 28291–28335, doi:10.1029/98JD02398, 1998. 29451

Horowitz, L. W., Walters, S., Mauzerall, D. L., Emmons, L. K., Rasch, P. J., Granier, C., Tie, X., Lamarque, J.-F., Schultz, M. G., Tyndall, G. S., Orlando, J. J., and Brasseur, G. P.: A global simulation of tropospheric ozone and related tracers: description and evaluation of MOZART, version 2, J. Geophys. Res., 108, 4784, doi:10.1029/2002JD002853, 2003. 29451

Kinnison, D., Johnston, H., and Wuebbles, D.: Ozone calculations with large nitrous oxide and chlorine changes, J. Geophys. Res., 93, 14165–14175, doi:10.1029/JD093iD11p14165, 1988. 29449

Lin, S.-J.: A "vertically Lagrangian" finite-volume dynamical core for global models, Mon. Weather Rev., 132, 2293–2307, 2004. 29451

Morgenstern, O., Giorgetta, M. A., Shibata, K., Eyring, V., Waugh, D. W., Shepherd, T. G., Akiyoshi, H., Austin, J., Baumgaertner, A. J. G., Bekki, S., Braesicke, P., Brühl, C., Chipperfield, M. P., Cugnet, D., Dameris, M., Dhomse, S., Frith, S. M., Garny, H., Gettelman, A., Hardiman, S. C., Hegglin, M. I., Jöckel, P., Kinnison, D. E., Lamarque, J.-F., Mancini, E., Manzini, E., Marchand, M., Michou, M., Nakamura, T., Nielsen, J. E., Olivié, D., Pitari, G., Plummer, D. A., Rozanov, E., Scinocca, J. F., Smale, D., Teyssèdre, H., Toohey, M., Tian, W., and Yamashita, Y.: Review of the formulation of present-generation stratospheric chemistry-climate models and associated external forcings, J. Geophys. Res., 115, D00M02, doi:10.1029/2009JD013728, 2010. 29452

Newman, P. A., Nash, E. R., Kawa, S. R., Montzka, S. A., and Schauffler, S. M.: When will the Antarctic ozone hole recover?, Geophys. Res. Lett., 33, L12814, doi:10.1029/2005GL025232, 2006. 29455

Oman, L. D., Plummer, D. A., Waugh, D. W., Austin, J., Scinocca, J. F., Douglass, A. R., Salawitch, R. J., Canty, T., Akiyoshi, H., Bekki, S., Braesicke, P., Butchart, N., Chipperfield, M. P., Cugnet, D., Dhomse, S., Eyring, V., Frith, S., Hardiman, S. C., Kinnison, D. E., Lamarque, J.-F., Mancini, E., Marchand, M., Michou, M., Morgenstern, O., Nakamura, T., Nielsen, J. E., Olivié, D., Pitari, G., Pyle, J., Rozanov, E., Shepherd, T. G., Shibata, K., Stolarski, R. S., Teyssèdre, H., Tian, W., Yamashita, Y., and Ziemke, J. R.: Multimodel assessment of the factors driving stratospheric ozone evolution over the 21st century, J. Geophys. Res., 115, D24306, doi:10.1029/2010JD014362, 2010a. 29454, 29455

Oman, L. D., Waugh, D. W., Kawa, S. R., Stolarski, R. S., Douglass, A. R., and Newman, P. A.: Mechanisms and feedback causing changes in upper stratospheric ozone in the 21st century, J. Geophys. Res., 115, D05303, doi:10.1029/2009JD012397, 2010b. 29460, 29461

Portmann, R. W. and Solomon, S.: Indirect radiative forcing of the ozone layer during the 21st century, Geophys. Res. Lett., 34, L02813, doi:10.1029/2006GL028252, 2007. 29449, 29450

Randeniya, L., Vohralik, P., and Plumb, I.: Stratospheric ozone depletion at northern mid latitudes in the 21st century: the importance of future concentrations of greenhouse gases nitrous oxide and methane, Geophys. Res. Lett., 29, 1051, doi:10.1029/2001GL014295, 2002. 29449

Ravishankara, A. R., Daniel, J. S., and Portmann, R. W.: Nitrous oxide (N_2O): the dominant ozone-depleting substance emitted in the 21st century., Science, 326, 123–125, doi:10.1126/science.1176985, 2009. 29449, 29450, 29454

Rayner, N., Parker, D., Horton, E., Folland, C., Alexander, L., Rowell, D., Kent, E., and Kaplan, A.: Global analyses of sea surface temperature, sea ice, and night marine air temperature since the late nineteenth century, J. Geophys. Res., 108, 4407, doi:10.1029/2002JD002670, 2003. 29452

Rex, M., Salawitch, R., von der Gathen, P., Harris, N., Chipperfield, M., and Naujokat, B.: Arctic ozone loss and climate change, Geophys. Res. Lett., 31, 4116, doi:10.1029/2003GL018844, 2004. 29458

Röckmann, T., Grooß, J.-U., and Müller, R.: The impact of anthropogenic chlorine emissions, stratospheric ozone change and chemical feedbacks on stratospheric water, Atmos. Chem. Phys., 4, 693–699, doi:10.5194/acp-4-693-2004, 2004. 29458

Rosenfield, J. E. and Douglass, A. R.: Doubled CO_2 effects on NO_y in a coupled 2-D model, Geophys. Res. Lett., 25, 4381–4384, doi:10.1029/1998GL900147, 1998. 29450, 29453

Rosenfield, J. E., Douglass, A. R., and Considine, D. B.: The impact of increasing carbon dioxide on ozone recovery, J. Geophys. Res., 107, ACH7-1–ACH7-9, doi:10.1029/2001JD000824, 2002. 29449

Shepherd, T. G.: Dynamics, stratospheric ozone, and climate change, Atmos. Ocean, 46, 117–138, doi:10.3137/ao.460106, 2008. 29454, 29460

SPARC CCMVal, SPARC Report on the Evaluation of Chemistry-Climate Models, edited by: Eyring, V., Shepherd, T. G., and Waugh, D. W., SPARC Report No. 5, WCRP-132, WMO/TDNo. 1526, available at: http://www.sparc-climate.org/publications/sparc-reports/sparc-report-no5/ SPARC, 2010. 29455, 29457, 29459

Stenke, A. and Grewe, V.: Simulation of stratospheric water vapor trends: impact on stratospheric ozone chemistry, Atmos. Chem. Phys., 5, 1257–1272, doi:10.5194/acp-5-1257-2005, 2005. 29449

Stolarski, R. S., Douglass, A. R., Newman, P. A., Pawson, S., and Schoeberl, M. R.: Relative contribution of greenhouse gases and ozone-depleting substances to temperature trends in the stratosphere: a chemistry-climate model study, J. Climate., 23, 28–42, doi:10.1175/2009JCLI2955.1, 2010. 29460

Tian, W. and Chipperfield, M. P.: A new coupled chemistry–climate model for the stratosphere: the importance of coupling for future O_3-climate predictions, Q. J. Roy. Meteor. Soc., 131, 281–303, doi:10.1256/qj.04.05, 2005. 29455

Tian, W., Chipperfield, M. P., and Lü, D.: Impact of increasing stratospheric water vapor on ozone depletion and temperature change, Adv. Atmos. Sci., 26, 423–437, doi:10.1007/s00376-009-0423-3, 2009. 29449

WMO: Scientific assessment of ozone depletion: 2006, World Meteorological Organisation, Global Ozone Research and Monitoring Project–Report, Geneva, Switzerland, 50, 572, 2007. 29449, 29455, 29460

Wuebbles, D. J.: Nitrous oxide: no laughing matter, Science, 326, 56–57, doi:10.1126/science.1179571, 2009. 29449, 29450, 29454

Wuebbles, D. J. and Hayhoe, K.: Atmospheric methane and global change, Earth-Sci. Rev., 57, 177–210, doi:10.1016/S0012-8252(01)00062-9, 2002. 29449

Xie, F., Tian, W., and Chipperfield, M. P.: Radiative effect of ozone change on stratosphere-troposphere exchange, J. Geophys. Res., 113, D00B09, doi:10.1029/2008JD009829, 2008. 29457

Table 1. The configurations of four CCM transient simulations.

Experiments	GHGs Scenario
E0	IPCC A1B scenario
E1	Linear 50 % increase in N_2O surface vmr from 2001–2050
E2	As E1 but with 100 % increase in N_2O 2001–2050
E3	As E1 with additional 50 % linear increase in CO_2 vmr from 2001–2050

Table 2. The configurations of four CCM sensitive simulations.

Simulations	GHGs Settings
S0	Fix N_2O as 2050 climatology in IPCC A1B scenario
S1	Increase N_2O by 50 % on S0 only in chemistry
S2	Increase N_2O by 50 % on S0 only in radiation
S3	Increase N_2O by 50 % on S0 interactively

Table 3. The tropical (25° N–25° S) upwelling (w^*) averaged between 70–20 hPa over the last 10 yr of the four simulations and changes in w^* (Δw^*) relative to the first 10 yr of the corresponding simulations.

Experiments	$w^*(10^{-3}\,\mathrm{m\,s^{-1}})$	$\Delta w^*(\%)$
E0	0.029	5.5
E1	0.032	28.4
E2	0.037	37.3
E3	0.033	21.9

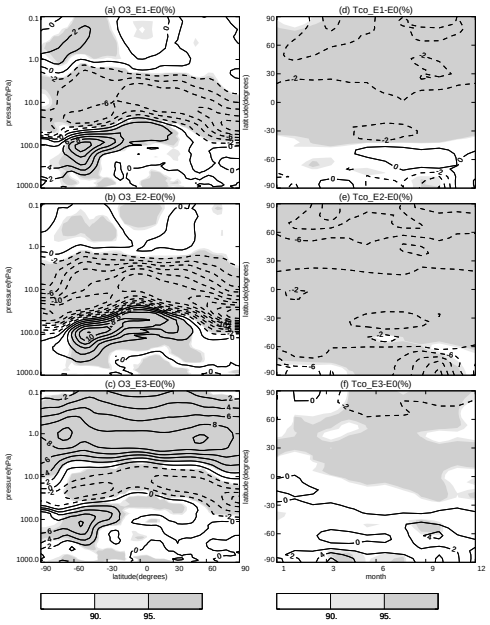

Fig. 1. Latitude-pressure cross sections of differences (%) in zonal mean ozone mixing ratios (2041–2050) between WACCM experiments **(a)** E1 and E0, **(b)** E2 and E0, and **(c)** E3 and E0. Time-latitude cross sections of differences (%) in zonal mean total column ozone climatology (2041–2050) between experiments **(d)** E1 and E0, and **(e)** E2 and E0, **(f)** E3 and E0. The contour interval is 2 % for percentage ozone changes. The grey colors represent significance levels for the mean state differences between different experiments by the Student's *T* test.

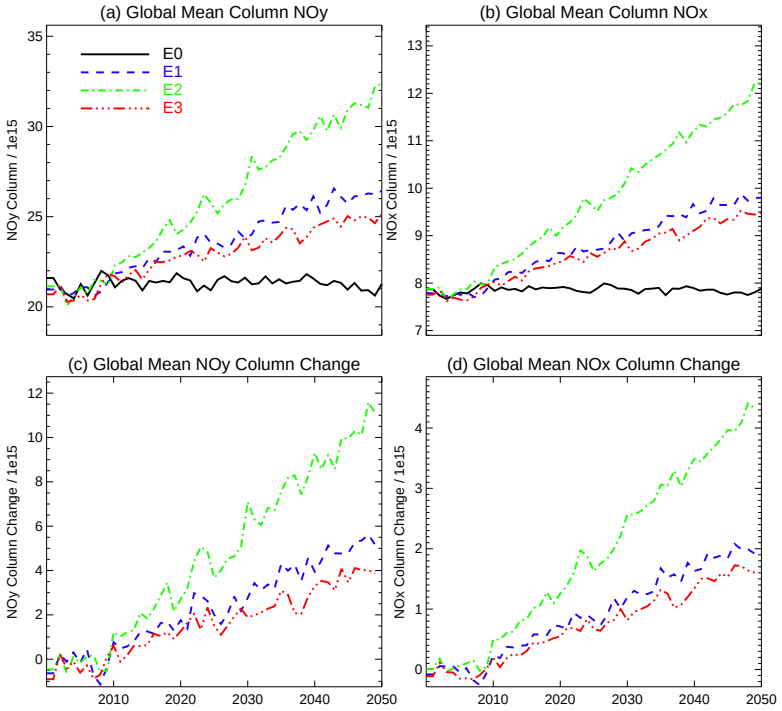

Fig. 2. Time series of global mean **(a)** column NO_y (molecules cm^{-2}) and **(b)** column NO_x (molecules cm^{-2}) in E0 (black line), E1 (blue line), E2 (green line) and E3 (red line). Difference in **(c)** column NO_y and **(d)** column NO_x between E1 and E0 (blue line), E2 and E0 (green line), E3 and E0 (red line).

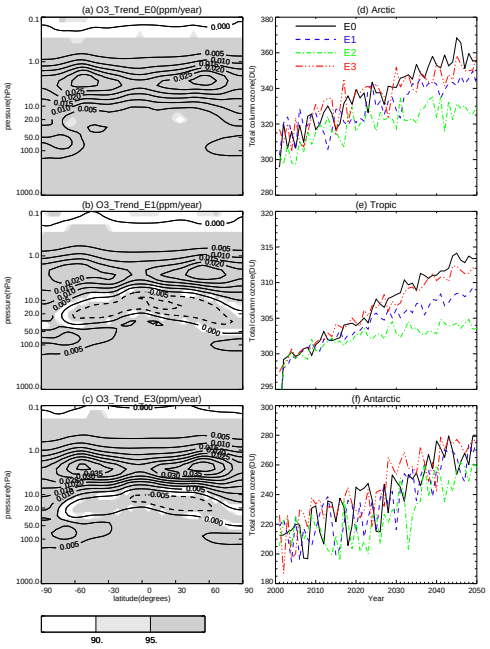

Fig. 3. (a, b, c) Latitude-pressure cross sections of the long-term (2001–2050) trends of zonal mean ozone mixing ratios (ppmv yr^{-1}) in WACCM experiments E0, E1 and E3. The contour interval is 0.005 ppmv yr^{-1}. Grey colors represent statistic significance levels of the trends. **(d, e, f)** Time series of total column ozone (DU) in different regions (Arctic, Tropics, Antarctic) in experiments E0 (black line), E1 (blue dashed line), E2 (green dashed-dotted line) and E3 (red dashed-dotted line).

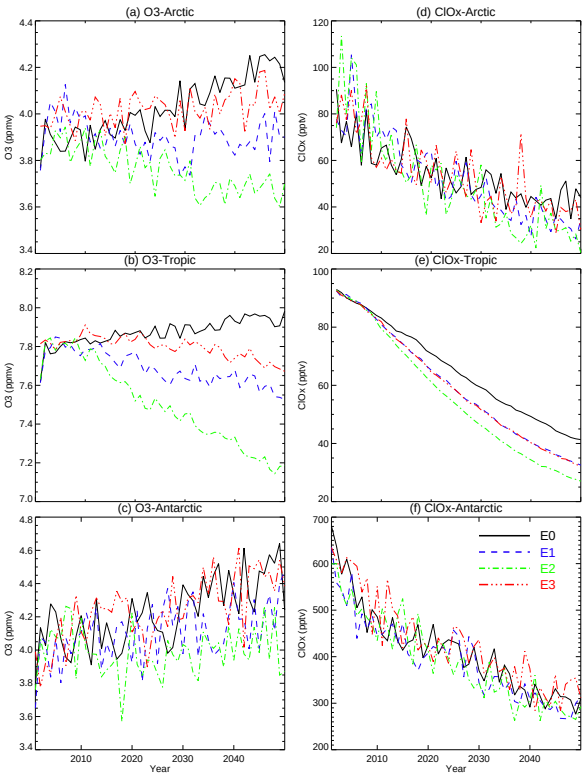

Fig. 4. Time series of mean **(a, b, c)** ozone and **(d, e, f)** Cl_x (Cl_x = Cl + ClO + 2 Cl_2O_2) between 20–10 hPa averaged over **(a)** Arctic (60° N–90° N), **(b)** Tropics (22° N–22° S) and **(c)** Antarctic (60° S–90° S) in E0 (black line), E1 (blue line), E2 (green line) and E3 (red line).

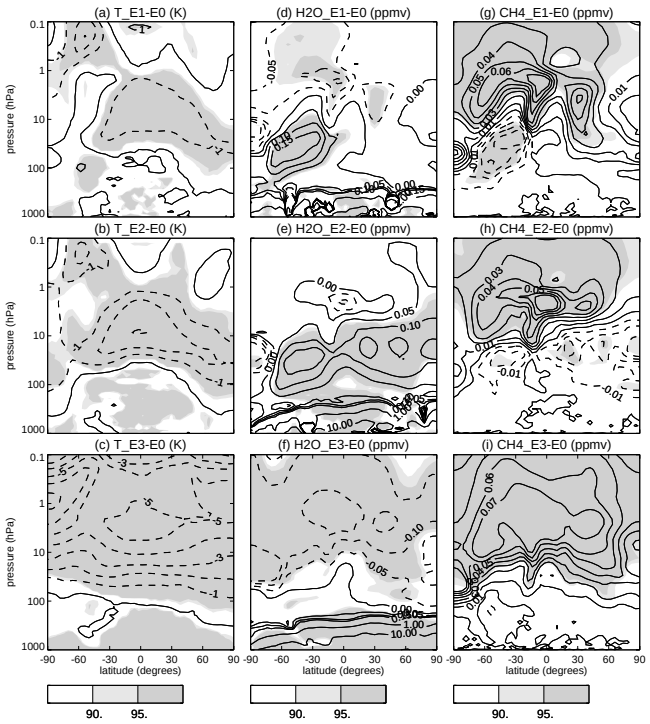

Fig. 5. Latitude-pressure cross sections of differences in **(a, b, c)** zonal mean temperature, **(d, e, f)** H_2O and **(g, h, i)** CH_4 climatology (2041–2050) between WACCM experiments. The contour intervals are 1 K for temperature, 0.01 ppmv for CH_4 and 0.05 ppmv for H_2O in the stratosphere where H_2O mixing ratios low. Grey colors represent statistical significance levels for the mean state differences between different experiments by the Student's *T* test.

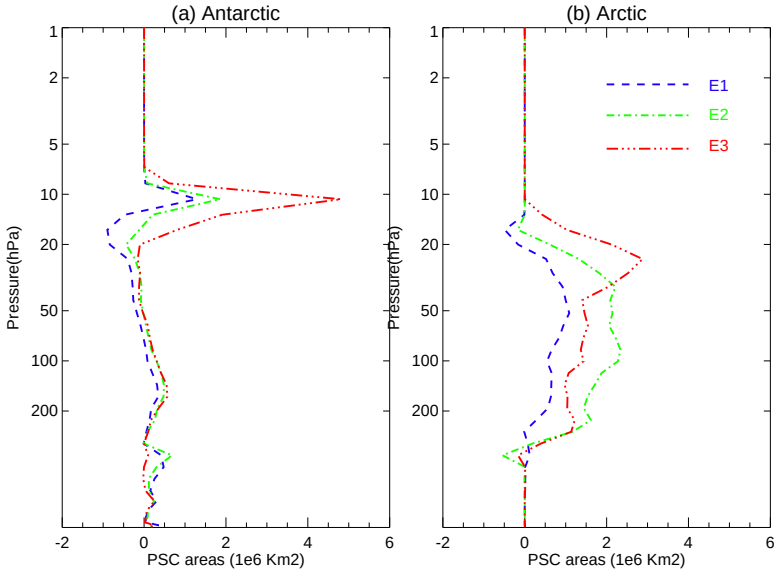

Fig. 6. Profiles of differences in annual mean PSCs area ($\times 10^6$ km^2) between WACCM experiments E1 and E0 (blue dashed line), E2 and E0 (green dashed dotted line), and E3 and E0 (red dashed dotted line) in **(a)** Antarctic and **(b)** Arctic.

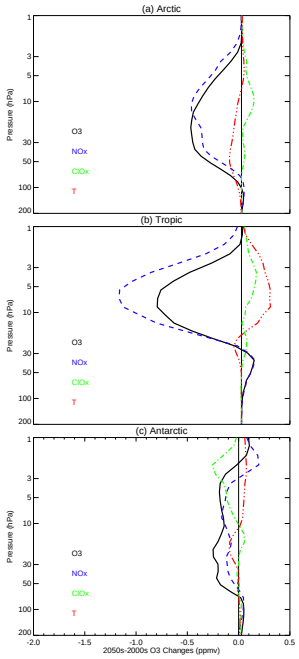

Fig. 7. Results of multiple regressions for spatially-averaged ozone change (ΔO_3 = O_3 (E1) $-O_3$ (E0)) with spatially-averaged NO_x, ClO_x and T change. The averaging domains are 90° N–70° N, 22° N–22° S, and 70° S–90° S. The black thick line shows the changes of ΔO_3 from 2001 to 2050 ($d\Delta O_3$), calculated by a simple linear regression of ΔO_3 with year ($\Delta O_3 = a_0 + a_1 \times$year, $d\Delta O_3$=a1 × 50). The blue dashed line, green dashed-dotted line and red dashed double point line show the NO_x, EESC and T contributions to ΔO_3 (i.e. $d\Delta O_{3,NO_x} = \Delta NO_x \times Coefs_{NO_x}$), respectively.

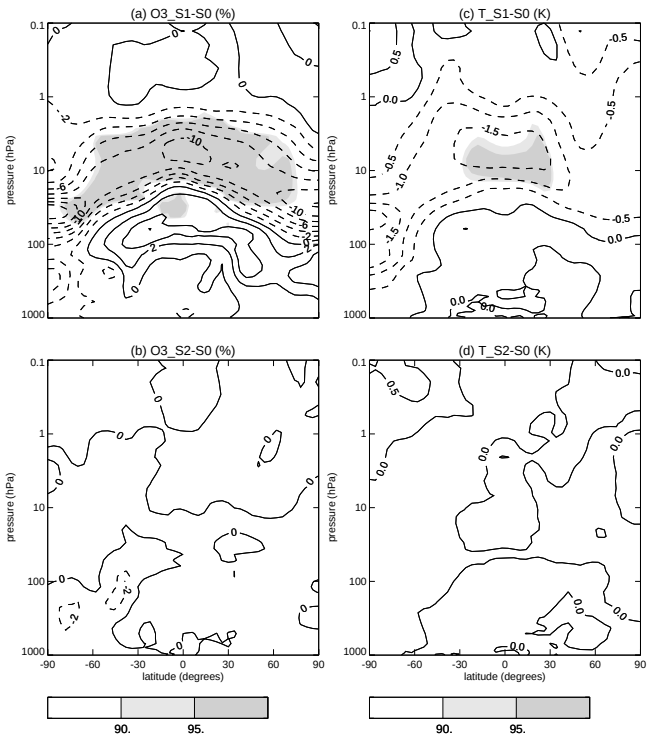

Fig. 8. Latitude-pressure cross sections of zonal mean ozone differences (%) between WACCM sensitivity experiments **(a)** S1 and S0, and **(b)** S2 and S0, and temperature differences (K) between sensitivity experiments **(c)** S1 and S0, and **(d)** S2 and S0. The contour interval for ozone is 2 % and for temperature is 0.5 K. Grey colors represent statistical significance levels for the mean state differences between different simulations by the Student's T test.

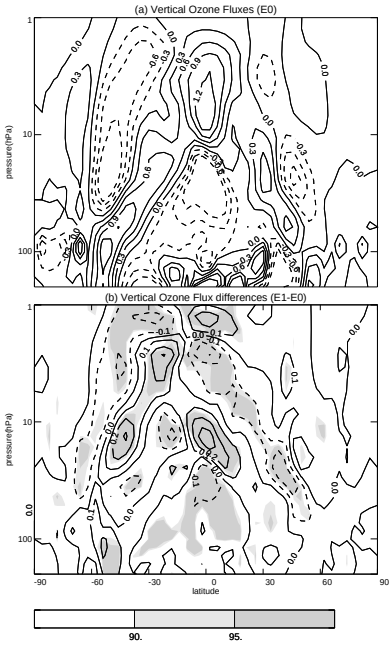

Fig. 9. Vertical ozone fluxes associated with the BD circulation (w^*) calculated from **(a)** reference experiment (E0) and **(b)** the differences between E1 and E0 (for more details of the definition of ozone flux see text). The contour intervals are $0.3 \times 10^3\,\mathrm{kg\,s^{-1}}$ and $0.1 \times 10^3\,\mathrm{kg\,s^{-1}}$ in **(a)** and **(b)**, respectively. Grey colors **(b)** represent the statistical significance levels for the mean state differences between different experiments by the Student's T test.